



## OPEN MGMT upregulation mediates Temozolomide resistance conferred USP5 dependency

Sachin Bhardwaj<sup>1,3</sup>, Sanjay<sup>1,3</sup>, Devansh Sharma<sup>1,3</sup>, Lakshay Taneja<sup>1</sup>, Birender K. Yadav<sup>2</sup> & Ajay Kumar Yadav<sup>1</sup>✉

Glioblastoma remains highly aggressive and has the ability to acquire resistance to Temozolomide, the standard chemotherapeutic agent. Deubiquitinating enzymes are emerged as critical regulators of tumor survival and drug resistance. Our study investigates the functional roles of MGMT, USP5, and USP8 in Temozolomide-resistant glioma, with a primary focus on the regulation of MGMT upon USP5 and USP8 intervention. Temozolomide-resistant cell lines U87 TMZ & LN229 TMZ were developed by treating cells with escalating dosages of upto 400  $\mu$ M TMZ in U87MG and LN229 upto 200  $\mu$ M TMZ, respectively. Expression analysis of DUBs was conducted using GEPIA2, GlioVis, and mRNA correlation studies of USP5, USP8, and MGMT were accessed through cBioPortal databases. Expression profiling of DUBs and MGMT was performed in established TMZ-resistant U87MG (400  $\mu$ M) and LN229 (200  $\mu$ M) glioma cells. The correlation between USP5 and MGMT expression was substantiated by siRNA-mediated knockdown of USP5 and USP8, led downregulation of MGMT, along with sensitization to apoptosis. Immunofluorescence staining was used to determine the subcellular co-localization of USP5 and MGMT in U87 TMZ-resistant glioma cells and in Grade IV glioma patient tumor tissue sections. Transcript expression of USP5 and MGMT was also assessed using glioblastoma microarray datasets ( $N=145$ ) from GEO database, data was visualized by drawing out heatmap chart, Z-score-based two-way contingency testing, and linear regression analysis. Transient ectopic overexpression of USP5 cloned plasmid was performed in U87MG glioma cells and HEK293T cells to assess its affect on MGMT protein expression. Comparative analysis between glioma tumor and non-tumor brain samples in GEPIA2 data showed USP1 and USP10 were significantly overexpressed, but USP5, USP7, USP8, and USP14 showed no significant differences. Therefore, we chose an additional database, GlioVis, where DUB family genes USP5, USP7, and USP14 were downregulated, possibly not carrying a Temozolomide-dependent resistance effect with only subtle variation observed. Consequently, further analysis of DUB proteins in LN229 and U87MG Temozolomide-resistant glioma cells was performed. In the cohort database, USP5 was positively correlated with MGMT mRNA (Pearson  $r=0.30$ ,  $p=0.04$ ), whereas most other USP family mRNAs were negatively correlated with MGMT. Western blot analysis of Temozolomide-resistant glioma cells (up to 400  $\mu$ M) showed that USP5, USP8, USP10, TNFAIP3, and MGMT, known resistance factors, were upregulated at protein levels in both U87 TMZ and LN229 TMZ-resistant glioma cells. Simultaneously, knockdown of USP5 or USP8 triggered apoptotic reactions in U87 TMZ-resistant cells, along with downregulation of MGMT and USP10 protein expression. Upregulation of SMAC (apoptotic protein) and LC3B-II reflected activation of apoptosis and autophagy after USP5 and USP8 knockdown. Treatment of Temozolomide-resistant cells with Bortezomib restored MGMT protein levels upon USP5 and USP8 knockdown, implying proteasome-mediated degradation of MGMT. Immunofluorescence staining established cytoplasmic co-localization of USP5 and MGMT in TMZ-resistant cells and Grade IV glioma tissue. Microarray-based GEO dataset analysis further demonstrated a significant positive correlation between USP5 and MGMT expression (Fisher's exact test  $p$ -value = 0.04). Notably, USP8 knockdown in U87 TMZ-resistant cells reduced MGMT expression without altering USP5 levels, as confirmed by immunofluorescence. Combining USP8

silencing with proteasome inhibition further diminished MGMT expression, revealing a novel USP5-independent role in stabilizing MGMT. Furthermore, USP5 overexpression in U87MG and HEK293T cells resulted in elevated MGMT protein levels, validating the significant correlation between USP5 and MGMT in glioma and other cancers. Additionally, MGMT-independent TMZ resistance was observed to be USP5- and USP8-dependent, preferably due to USP10 upregulation. Both USP5 and USP8 play pivotal but distinct roles in mediating Temozolomide resistance in glioma by sustaining MGMT protein expression. USP5 enhances MGMT expression through direct interaction, while USP8 maintains MGMT stability independent of USP5. Targeting USP5 or USP8 represents a promising strategy to overcome chemoresistance and may enhance glioma treatment efficacy.

**Keywords** USP5, USP8, USP10, MGMT, Apoptosis, Temozolomide, Bortezomib

#### Abbreviations

DUB	Deubiquitinating enzyme
USP5	Ubiquitin Specific Protease 5
USP1	Ubiquitin Specific Protease 1
USP8	Ubiquitin Specific Protease 8
USP10	Ubiquitin Specific Protease 10
USP7	Ubiquitin Specific Protease 7
TMZ	Temozolomide
MGMT	O <sup>6</sup> Methyl Guanine DNA Methyl Transferase

<sup>1</sup>Molecular Cancer Genetics and Signal Transduction Laboratory, Dr. B.R Ambedkar Centre for Biomedical research, University of Delhi, North Campus, Gate No. 1, Vishwavidyalaya Marg, Mall Road, 44, AH2, Delhi 110007, India. <sup>2</sup>Rajiv Gandhi Cancer Institute and Research Centre (RGIRC), New Delhi, India. <sup>3</sup>Sachin Bhardwaj, Sanjay and Devansh Sharma contributed equally to this work. ✉email: ayadav@acbr.du.ac.in; ajayacbrdu@gmail.com; ajay9774@gmail.com

Glioblastoma is a lethal brain tumor with limited treatment modalities, is typically managed with surgical removal followed by adjuvant radiotherapy and chemotherapy using the alkylating drug Temozolomide (TMZ). Temozolomide among the chemotherapy has good anti-tumor activity and limited toxicity which gives survival benefit to GBM patient with median survival 18 months, where O<sup>6</sup>-methyl guanine DNA methyltransferase (MGMT) promoter is methylated. Tumor resistance to Temozolomide is frequently observed in patients whose tumors exhibit an unmethylated MGMT promoter. By removing the cytotoxic alkyl group from DNA, the MGMT protein effectively counteracts the therapeutic effect of TMZ, leading to rapid development of a resistant phenotype and, consequently, diminished patient survival<sup>1</sup>.

MGMT CpG island upon methylation influences the MGMT gene expression located downstream of the transcription start site (TSS) about 130 nucleotides (+130) and also located upstream –252 to –155 and –90 to +65 found that 21 out of 25 loci were negatively correlated with MGMT expression. Moreover, across the cell lines HT29 (expressing MGMT) and BE (not expressing MGMT), including glioma xenografts and normal brain tissue, it was found that methylation of CpG at –186 to –172 and +93 to +153 regions were the key regions and were mostly correlated with MGMT gene expression<sup>2</sup>, and further it was found that +152 to +214 were the key region promoting the MGMT transcription<sup>3</sup>. The methylation status of MGMT promoter which silences MGMT expression were reported as prognosis predictor. Upon expression of the unmethylated MGMT promoter, TMZ induced O<sup>6</sup>-methylated guanine adducts were removed, conferring TMZ resistance in approx. 60% GBM patient.

Furthermore, chemotherapy and radiotherapy significantly influences MGMT promoter methylation activity, with more pronounced changes observed in recurrent tumors from patients who initially had a methylated MGMT promoter compared to those with an unmethylated promoter. This alteration in methylation status, in turn, affects the expression of the MGMT protein<sup>4</sup>. In another study MGMT methylation status in 89% was not altered in group of 16 patients with radiotherapy only and 64 patients with radiotherapy + Temozolomide chemotherapy. This noted the low response of MGMT promoter against the effectivity of DNA damaging agent in group of patients<sup>5</sup>. This further identified that glucocorticoids also promote MGMT expression, in addition to a genotoxic stress<sup>6</sup>, in retrospective clinical data with no glucocorticoids tends longer survival in malignant glioblastoma patients<sup>7</sup>. Thus, additional factors along with radiation or Temozolomide play a role in MGMT expression. Though the route behind TMZ mediated resistance is majorly MGMT expression. The glioma cancer stem cells in cell line model were seen getting sensitized to TMZ due to gradual loss of MGMT upon obtaining its differentiation state<sup>8,9</sup>.

Functionally, MGMT (O<sup>6</sup>-Methyl guanine-DNA methyl transferase) during DNA break repair, specifically transfers alkyl adducts from the O<sup>6</sup> position of guanine to its cysteine residue (Cys 145) in active site. This irreversible binding causes inhibition of its MGMT enzyme activity leading to protein ubiquitylation or degradation. These protein ubiquitylation phenomena is a three step process comprising of: ubiquitin activating enzyme (E1), ubiquitin-conjugating enzyme (E2), and ubiquitin ligase (E3) in a sequential way placing a ubiquitin to the lysine of a target protein. Target protein ubiquitylation depending upon the nature of ubiquitin type determines the fate of a target proteins. At the same place another class of Deubiquitinating enzymes family protein imparts a key role by removing the ubiquitin from targeted ubiquitylated proteins. MGMT expression and its degradation is a key regulatory function to bring mechanistic insights behind the existence of MGMT in low or high abundance is not understood. UBE2B E3 ligase exhibited the interaction with MGMT in BCNU,

Cisplatin and Tamoxifen induced ubiquitin dependent proteolysis of MGMT in numerous types of tumors were studied. The E3 ligase RAD18 as an interacting partner of UBE2B is also involved in BCNU mediated MGMT ubiquitination<sup>10</sup>, the ubiquitin dependent degradation of MGMT is also by TRIM72 E3 ligase where, O6-methylguanine DNA methyl transferase (MGMT) is involved in chemo resistance against Dacarbazine (DTIC) treatment. The protein level of MGMT and TRIM72 was found negatively correlated, overexpression of TRIM72 degrades the MGMT and showed increased sensitivity to DTIC treatment<sup>11</sup>.

Recently, it was discovered that Deubiquitinating family enzymes protein play a critical role in Glioma growth by stabilizing FLIPS and TRAIL ligand sensitivity<sup>12</sup>, PML tumor suppressor suppression<sup>13</sup>, increased c-MYC activity downstream of p53 and PTEN mutation enhances the self-renewal capacity of GBM tumor initiating cells<sup>14,15</sup>, where c-MYC desumoylation<sup>16</sup> and its deubiquitylation are further key modifiers in cancer cell proliferation<sup>17–20</sup>. USP5, a DUB family protein sustains the proliferation of glioma cells through stabilization of Cyclin D1<sup>21</sup>. USP5 emerges as a promising pan-cancer biomarker, showing strong diagnostic accuracy (AUC > 0.9 in several tumors) and association with poor patient prognosis. Beyond its diagnostic value, USP5 modulates the tumor immune microenvironment by correlating with immune-regulatory genes such as LAG3, CD4, PD-1, PD-L1 highlighting its role in tumor-immune interactions<sup>22</sup>. E2F1, a transcription factor regulates USP5 mediated deubiquitination of OCT4 in mesenchymal glioma stem cells (MES GSC's) and its maintenance<sup>23</sup>. However, in glioma cell lines USP5 down regulation doesn't allow inhibition in cell growth or apoptosis induction, similarly USP8 knock down doesn't increase apoptosis, unless there is a co-knockdown of both USP5 and USP8 in U87MG or in LN229<sup>24</sup>.

In present study the aberrant expression of USP5 causing MGMT independent or dependent effect in the presence of Temozolomide in U87MG and LN229 glioma cell lines with acquired TMZ resistance, was extended to elucidate the DUB family proteins in combination to add on the pivotal association in resistance development. Further the aim is to study the association of low or high MGMT expression and its co-localization effect with Deubiquitinating enzyme family protein USP5 in presence or absence of USP8 was investigated.

## Materials and methods

### Cell culture

Glioma cells U87 MG and LN229 were purchased from the National Centre for Cell Science, Pune, India (known cell line supplier). Development of Temozolomide resistant were described previously<sup>25</sup>. Temozolomide-resistant cells (U87MG TMZ) were developed by treating cells with TMZ in an escalated dosage of up to 400  $\mu$ M TMZ. Drug-resistant and non-resistant glioma cell lines with passages 20 were grown in Dulbecco's modified Eagle's medium (DMEM) (Himedia) in the presence or absence of the given drug, along with 10% fetal bovine serum (Himedia) and 100 unit's/ml penicillin–streptomycin (Gibco), at 37 °C in a humidified chamber under 5% CO<sub>2</sub>. Temozolomide was purchased from Sigma-Aldrich(T2577).

### SiRNA transfection

U87 MG TMZ and LN229 resistant glioma cells (2 × 10<sup>4</sup> cells) were seeded and after 17 h of plating, cells were transfected with two siRNA specific for USP5 (10nM) and USP8 (10nM) using Interferrin transfection reagent (Polyplus) as per protocol. USP5 (1) sequence was 5'- GAUGGGUGAUCUACAAUGA-3' & USP5 (2) 5'-CUGA GUUGGAGAUAGACAU-3' and USP8 (1) sequence was 5'- CAGGACAGUAUAGAUUAU-3' & USP8(2) 5'-U AAAUGGCUUGCCUGAACC-3'. After 72 h of transfection protein lysates were prepared in a cell lysis buffer (Cell signaling) containing protease inhibitors (Abcam) and phosphatase inhibitors (Sigma). siRNA-mediated knockdown efficiency was found  $\geq$  50% to 60% in USP5(1) and USP8 (1), based on western blot data, so after analyze knockdown efficiency USP5 (1) and USP8 (1) siRNA were used in further experiments.

### Western blotting and antibodies

U87 MG TMZ and LN229 TMZ resistant glioma cells (2 × 10<sup>6</sup>) were seeded and grown in TMZ media for 72 h. Total protein lysates were made from SDS-cell lysis buffer (Cell Signaling Technology). The protein concentration was determined by the Bradford reagent (BioRad). The total protein of concentration 50  $\mu$ g was subjected to 8–12% sodium dodecyl sulfate-polyacrylamide gel electrophoresis and transferred onto a PVDF (MDI) membrane at 20 V overnight at room temperature. The next day, membranes were blocked with 5% non-fat dry milk for non-phosphorylated proteins or blocked with 5% BSA for phosphorylated proteins for 1 h. After this, the membrane was washed using Tris-buffered saline with Tween 20 3 times (5 min each) and processed for specific primary antibodies overnight at 4 °C. The primary antibodies against anti- USP5(Proteintech, 10473-1-AP, 1:10000), USP1(Proteintech, 14346-1-AP, 1:10000), USP7(Cloude clone Corp, PAC255Hu01, 1:2500), USP10(Proteintech, 19374-1-AP, 1:10000), USP14(Proteintech, 14517-1-AP, 1:10000), anti- LC3B (abcam, 1:2500), anti-SMAC (Abcam, ab32023, 1:2500), USP8 (Proteintech, 1:10000, 67321-1-Ig), anti-TNFAIP3 (abcam, ab92324, 1:2500), MGMT and anti- $\beta$ -actin (Biospes, BTL1027, 1:5000). Followed by probing with specific secondary antibody (1:5000) for 1 h and developed using Chemiluminescent reagent (Bio-Rad), under Chemiluminescent Gel Documentation system. Horseradish peroxidase conjugated secondary antibodies (anti-mouse, GeNei, 114068001 A, and anti-Rabbit, GeNei, 114038001 A) were used.

### Deubiquitinating enzymes gene expression survival analysis using the GEPIA 2 and gliovis webserver

To investigate Deubiquitinating enzymes (USP1, USP5, USP7, USP8, USP10, USP14) gene expression in glioma tumor compared with normal matches, we used the GEPIA 2 webserver (a webserver which extracts data from the Cancer Genome Atlas (TCGA) data portal and the GTEx database of normal tissues <http://gepia.cancer-pku.cn>) and Gliovis (<https://gliovis.bioinfo.cnio.es/>) web server. Regarding parameter options, we used the ANOVA statistical method for differential gene expression analysis, selected log<sub>2</sub>(TPM + 1) transformed expression

data for plotting, TCGA tumors compared with TCGA normal and GTEx normal for matched normal data in plotting,  $|\log_2FC|$  cutoff of 1, and a q-value cutoff of 0.01.

### cBioportal database and correlation expression

Integrative analysis of Glioblastoma was performed using cBioportal (<https://www.cbioportal.org/>), a publically available database for tumor genomics and transcriptomic analysis. Using the cBioportal database, we assessed the Glioblastoma (TCGA, Cell 2013) study; acquired data of 592 patients for mRNA correlation analysis of Ubiquitin Specific protease (USP) family of Deubiquitinating enzymes vs. MGMT.

### Microarray based gene expression analysis and linear regression analysis

In order to investigate gene expression profiles in glioblastoma (GBM), four microarray datasets publicly available were downloaded from the NCBI GEO database: GSE43378, GSE4412, GSE279426, GSE13041 consisting of a total of 145 GBM samples (Untreated patient tumours i.e. no treatment was given to the patient and the tumour was resected). From these datasets, a data table was created obtaining microarray probe values of the following genes of interest: USP5 (Probe ID: 206031\_s\_at) and MGMT (204880\_at). The respective Affymetrix probe IDs were retrieved from the BioGPS platform for precise mapping. For comparison and normalization among samples of the various datasets, raw expression levels for each gene in each dataset were converted to z-scores. This was performed independently for each dataset by first computing the mean and standard deviation of the expression levels and then applying the following z-score formula:  $z = (\text{value} - \text{mean}) / \text{standard deviation}$ . Then, to explore expression dynamics under varying states of gene expression, the dataset of the complete 145 GBM samples was aligned from the lowest z score value to the highest z score value of the USP5 samples. Based on these z-score values, heat maps were produced for the visualization of the expression trends USP5 & MGMT. Heat maps were produced using Heatmapper.ca, applying average linkage as the clustering strategy and Euclidean distance as the measure of similarity. This helped in comparative visualization of expression patterns between high expressers and low expressers of USP5 across all datasets, helping to identify co-regulatory relations and differential expression trends between USP5 and MGMT. The dataset ( $n = 145$ ) was divided into four different subsets HIGH USP5 ( $z > 0.2$ )-HIGH MGMT ( $z > 0.2$ ) ( $n = 31$ ); HIGH USP5 ( $z > 0.2$ )-LOW MGMT ( $z < 0.2$ ) ( $n = 26$ ); LOW USP5 ( $z < 0.2$ )-HIGH MGMT ( $z > 0.2$ ) ( $n = 32$ ); LOW USP5 ( $z < 0.2$ )-LOW MGMT ( $z < 0.2$ ) ( $n = 56$ ) and a contingency table was made to perform Fisher's exact test (two-tailed) using Graph Pad Prism. Linear regression plot was also made of the same sample ( $n = 145$ ) using Graph Pad plotting USP5 ( $n = 145$ ) v/s MGMT ( $n = 145$ ).

### Overall survival analysis of glioma patients using GEO expression datasets based on USP5-MGMT high/low expression groups

Out of these four datasets, three datasets, GSE43378, GSE4412 and GSE13041 ( $n = 131$ ), containing complete patient survival information were selected for analysis.

Patients were categorised based on gene expression profiles into two comparison groups: Positive correlation analysis: High USP5–High MGMT ( $n = 27$ ) vs. Low USP5–Low MGMT ( $n = 54$ ); Negative correlation analysis: High USP5–Low MGMT ( $n = 23$ ) vs. Low USP5–High MGMT ( $n = 27$ ); (HIGH =  $> 0.2$ ; LOW =  $< 0.2$ ). For each group, patient survival time (in days) and survival status [alive(0) or deceased(1)] were recorded. Kaplan–Meier survival analysis was performed using the StatsKingdom online Kaplan–Meier tool (<https://www.statskingdom.com/kaplan-meier.html>) with a 95% confidence interval. Survival time and event-status data (0 = censored, 1 = death) were extracted from the clinical dataset. For time intervals of 500 days each, the “number at risk” table was calculated as the total number of individuals who were still under observation and had not died yet. “Deaths” represent the number of patients who died within that interval. “Censored” cases refer to patients who remained alive by the last follow-up time, and they were removed from the risk set at the time of censoring.

### Correlation of USP5 expression with immune filtration in GBM using GSCA

Immune infiltration data were retrieved from the Gene Set Cancer Analysis (GSCA) platform (<http://bioinfo.life.hust.edu.cn/GSCA/>). GBM samples were stratified based on USP5 copy number variation (CNV) status, comparing wild-type (WT) with deleted groups.

GSCA's immune filtration and GSVA module was used to estimate the association between immune cells infiltrates and gene set expression level and other module was immune filtration and gene set CNV module to estimate the relative abundance of 24 immune subsets, including CD4<sup>+</sup> and CD8<sup>+</sup> T cells, regulatory T cells, T helper subtypes, NK cells, dendritic cells, neutrophils, and monocytes.

Group differences were assessed using the Wilcoxon rank-sum test and one-way ANOVA. Log<sub>2</sub> fold change values were calculated for each immune subset, and significance was defined as  $p < 0.05$ .

### Immunocytochemistry staining

U87 MG TMZ resistant cells were seeded on a 12 mm coverslip and after 17 h of plating, cells were transfected with siRNA specific for USP5 (10nM) and USP8 (10nM) using Interferrin transfection reagent (Polyplus) as per protocol. After 48 h of transfection, cells were treated with Bortezomib (50μM) for 24 h. Remove culture media and gently wash with ice-cooled 1x PBS for 5 min. Fix with 4% paraformaldehyde in PBS for 15 min at room temperature. Permeabilize samples with 5% BSA in PBS for 30 min after washing with 1xPBS. Aspirate blocking buffer and incubated with MGMT primary antibody (1:100 Proteintech, 67476-1-Ig) overnight at 4 degrees. Washed with PBS three times for 5 min and incubated with secondary antibody (Alexa flour 564- Abcam, ab150108, 1:250) for 1 h at room temperature. Mounted slides with a drop of mounting media containing DAPI (blue stain) and observed under the fluorescence microscope using 20 x lenses.

### Immunohistochemistry in glioblastoma grade IV tissue sections

Glioblastoma Grade IV paraffin embedded tissue sections slides were collected from Tissue Bio Bank of the Rajiv Gandhi Cancer Institute and Research Center (RGCIRC), New Delhi, Delhi. Additionally, all tumor tissue samples were approved by Human Ethic Committee approved as per its guidelines. RGCIRC ethical consent number - Res/SCM/17/2016/59 & ethical consent number of Dr. B R Ambedkar Centre for Biomedical Research, the place for conducted tissue sample analysis- ACBR/16/2379. These two GBM paraffin embedded tumor slides were obtained from the Tumor Tissue bank of Rajiv Gandhi Cancer Institute and Research Center (RGCIRC), New Delhi, Delhi. Protocol is as follows: Paraffin-embedded sections were routinely deparaffinized with xylene, rehydrated through a graded alcohol series, and followed by antigen retrieval at 95° C for 30 min, further incubated in 0.5% (v/v) hydrogen peroxide followed by 3 times washing with 1X PBS. After this, sections were incubated with 5% (v/v) Bovine Serum Albumin (BSA) for 45 min at room temperature. Sections were incubated with a primary antibody (USP5 (1:100 Proteintech, 10473-1-AP) & MGMT (1:100 Proteintech, 67476-1-Ig) at 4 °C in a humidified chamber overnight, followed by 4 times washing with 1X PBS. After that sections were incubated with Alexa Flour 594 Mouse secondary antibody (1:250) (Abcam, ab150108) and Alexa Flour 454 Rabbit secondary antibody (1:250, Thermofisher, A32731) for 2 h at room temperature. Washing was done 3 times with 1X PBS. In addition, any nuclear staining was confirmed with the DAPI staining under fluorescence microscope.

### Flow cytometric analysis of apoptosis by FITC-Annexin V/PI

Fluorochrome- labeled Annexin V-APC was used as a probe to detect exposed translocated membrane phospholipid as an indicator of early onset apoptosis for flow cytometry analysis. Propidium iodide (PI) was used in conjunction with Annexin V-APC staining to differentiate the apoptotic stages of the cells. U87 MG TMZ and LN229 TMZ resistant cells were transfected with specific siRNA (CNT (10nM), USP5 (10nM), USP8 (10nM)) for 72 h. Cells were harvested, washed twice with cold 1X PBS and then re-suspended in 100 µL of binding buffer. 100 µL of the solution was transferred to a FACS tube, followed by the addition of 5 µL of APC-conjugated Annexin V and 5 µL of Propidium iodide PI (Elabsience, Annexin-V APC apoptosis detection kit: E-CK-A217). The cells were gently vortexed and incubated for 20 min at room temperature, in the dark. Following this, 400 µL of binding buffer was added to each tube, and the samples were analysed by flow cytometry (FACS Calibur flow cytometer, BD Biosciences, San Jose, CA, USA) to examine the early and late stages of apoptosis. Each sample was analysed using Cell Quest Pro software (BD Biosciences, San Jose, CA, USA).

### Transient USP5 overexpression in HEK 293T cells

To investigate the effect of USP5 overexpression, full length USP5 transcript from CDS region was amplified by polymerase chain reaction by Phusion Plus High Fidelity DNA polymerase (Thermo Fisher, F630S). The sequence of primer used for full length USP5 transcript amplification is as follows: Forward Primer – 5' GTGGA GAAGCTGCTGCCG 3'; Reverse Primer – 5' CCCCTCTCCCTCATGCCA 3', cycling conditions are as follow: Initial denaturation at 95° C for 1 min, Denaturation at 95 °C for 10 s, Annealing at 60° C for 30 s and Extension at 72 ° C for 2 min for 30 cycles. The amplified gene after its respective restriction endonuclease digestion step, was ligated into the pBABE mammalian expression vector. U87 MG and HEK293T cells were seeded in 60 mm petri dishes upto ~ 70% confluency prior to USP5 plasmid transfection. Transient transfection of USP5 was performed in HEK293T using the calcium chloride (CaCl<sub>2</sub>) precipitation method. As per manufacturer protocol, a DNA-CaCl<sub>2</sub> mixture containing either pBABE-USP5 plasmid or empty pBABE vector (control) was prepared and added dropwise to a 2× HEPES-buffered saline (HBS) solution while gently vortexing. The resulting transfection complex was incubated for 20 min at room temperature to allow precipitate formation, followed by dropwise addition onto HEK293T cells. Cells were incubated with the transfection mix for 6–8 h, after which the medium was replaced with fresh complete DMEM. Cells were harvested 48 h post-transfection for protein analysis.

### Transient USP5 overexpression in U87 MG glioma cells

U87 MG glioma cells were seeded in 60 mm petri dishes 2 × 10<sup>4</sup>. After 17 h of plating, cells were treated with USP5 plasmid using Lipofectamine 3000 (Thermo Fisher Scientific) following the manufacturer's guidelines optimized for adherent cell lines. 5 µg of USP5 plasmid was complexed with Lipofectamine 3000 and P3000 reagent in serum-free medium, incubated for 20 min at room temperature and then added to the petri plates. After 24 h of transfection, the medium was refreshed with complete growth medium. Experimental groups included target plasmid transfections, along with mock (reagent only) and pBABE plasmid controls.

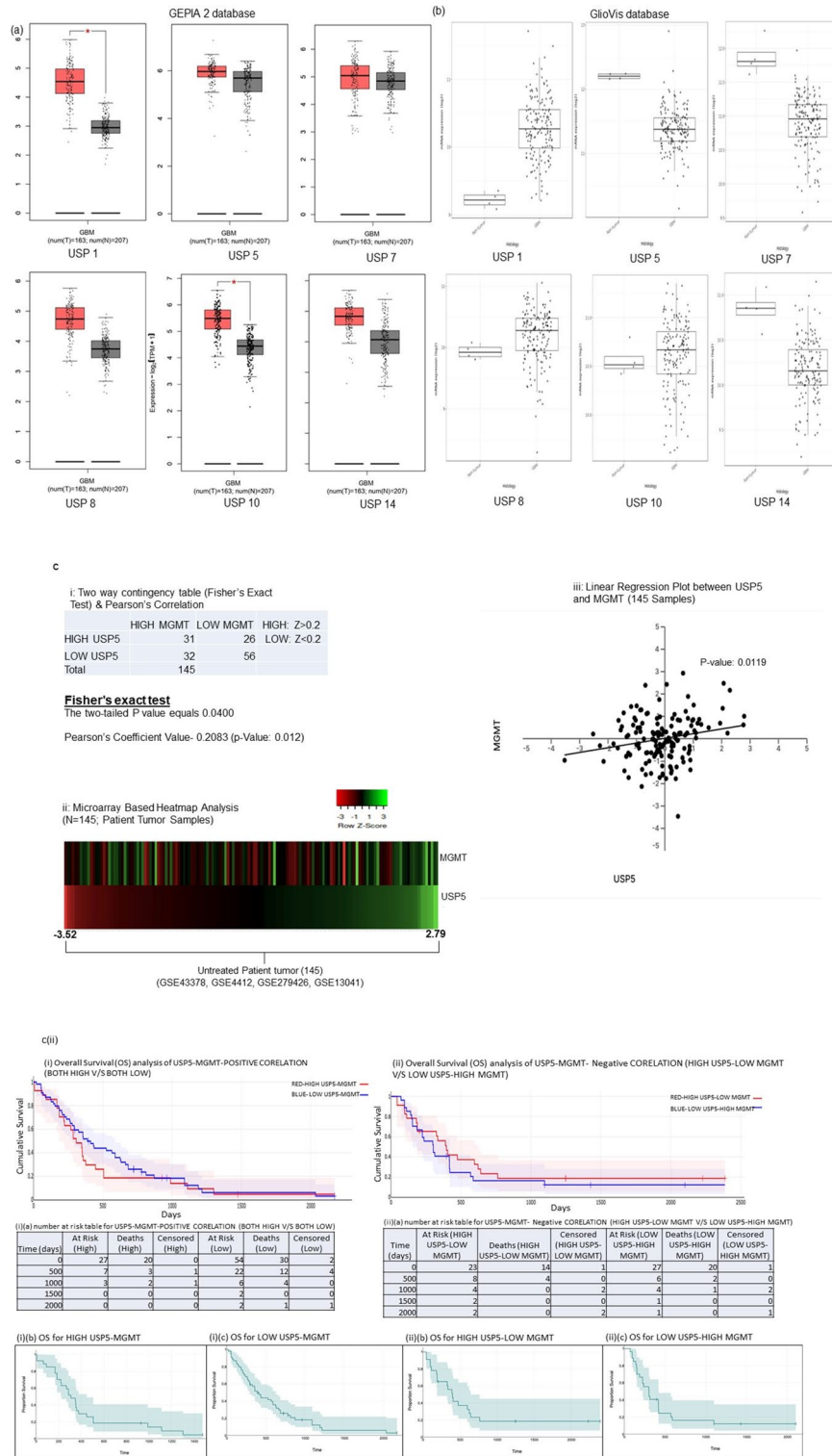
### Statistical analysis

The statistical analysis was assessed with the one-way or two-way ANOVA for comparison of data of more than two groups in the study conducted. Fisher's exact t-test (two-tailed) were performed for the contingency table. The student t-test unpaired was used for comparison of the two groups only. The p-value < 0.05(\*), < 0.01(\*\*), < 0.001(\*\*\*) , < 0.0001(\*\*\*\*) are considered significant.

## Result

### Deubiquitinating enzyme expression in glioma

Data extracted from the GEPIA 2 database, which assessed TCGA (The Cancer Genome Atlas) and GTEx databases covering glioma tumors matched with normal brain tissues, revealed that expression levels of deubiquitinating enzymes USP1 and USP10 were significantly overexpressed in GBM samples (*n* = 163) compared with non-tumor brain samples (*n* = 207). The TCGA data indicated that expression of USP8 and USP14 was also elevated in glioma tumors compared to normal brain tissues, but these differences were not statistically significant, whereas the expression of USP5 and USP7 showed no difference (Fig. 1a).



We accessed mRNA expression data of DUBs (USP1, USP5, USP7, USP8, USP10, USP14) from another database, GlioVis, which showed that deubiquitinating enzymes USP1 and USP8 were overexpressed, whereas USP5, USP10, USP7, and USP14 were downregulated in glioma tumors compared to normal brain tissue (Fig. 1b). This dataset concludes that mRNA expression of different DUBs varies between GEPIA and GlioVis databases, except for USP1, which is significantly overexpressed in both. This difference may depend on the acquired cohort set. Importantly, while the basal levels of USP5, USP8, and USP10 mRNA may not follow the same overexpression pattern, their encoded proteins and interacting signaling proteins were observed to be highly activated in proliferating glioma cell lines, particularly upon temozolomide treatment, as demonstrated in subsequent experimental data.

◀ **Fig. 1.** The expression level of deubiquitinating enzymes in glioma patients (data accessed through GEPIA 2 and GliVis) and in U87 MG and LN229 glioma cells. **(A)** Comparative expression of deubiquitinating enzymes (USP1, USP5, USP7, USP8, USP10, USP14) between GBM tumor samples ( $n=163$ ) and non-tumor samples ( $n=207$ ) analyzed using the GEPIA2 web tool. Red represents tumor samples and grey represents non-tumor samples. **(B)** Expression profiles of deubiquitinating enzymes (USP1, USP5, USP7, USP8, USP10, USP14) in GBM samples analyzed using the GliVis web tool. **(C)** (i) Microarray based comparison of gene expression data from Geo Expression Omnibus dataset between USP5 and MGMT and their linear regression. Statistical analysis was performed using Fisher's exact test and Chi square without Yates correction for two-way contingency table. P-value less than  $p < 0.05$ ,  $**p < 0.01$ ,  $***p < 0.001$  are considered significant. (ii) The patients were stratified into High USP5–High MGMT, Low USP5–Low MGMT, high USP5–low MGMT and low USP5–high MGMT groups based on z score values (HIGH =  $> 0.2$ ; LOW =  $< 0.2$ ). (iii) shows Kaplan–Meier overall survival curve showing positive correlation between USP5 and MGMT expression, comparing between patients with high expression of both USP5 and MGMT (red line), demonstrating poorer overall survival relative to those with low expression of both genes (blue line), (i)(a) shows the numbers at risk table of patients, where “at risk” denotes patients still alive and under observation, “deaths” represent mortality events, and “censored” corresponds to patients alive at the last contact comparing between patients with high expression of both USP5 and MGMT and low expression of both genes at 500 days intervals, (i)(b) & (i)(c) denotes the individual OS graph of patients with high expression of both USP5 and MGMT and low expression of USP5 and MGMT respectively. (ii) shows Kaplan–Meier overall survival curve showing negative correlation between USP5 and MGMT expression comparing between patients with high-USP5 & Low-MGMT expression (red line) and low-USP5 & high-MGMT expression (blue line), (ii)(a) shows the numbers at risk table of patients where “at risk” denotes patients still alive and under observation, “deaths” represent mortality events, and “censored” corresponds to patients alive at the last contact, comparing between patients with high-USP5 & Low-MGMT expression and low-USP5 & high-MGMT expression at 500 days intervals, (ii)(b) & (ii)(c) denotes the individual OS graph of patients with high-USP5 & Low-MGMT expression and low-USP5 & high-MGMT expression respectively. **(D)** mRNA expression correlation analysis between USP5/USP8 and MGMT genes using cBioPortal with the Glioblastoma (TCGA, Pan Cancer Atlas) dataset. Y-axis represents mRNA expression levels of USP5; X-axis represents mRNA expression levels of MGMT gene. **(E)** Tabulated correlation coefficients for mRNA expression between ubiquitin-specific proteases (USPs) and MGMT gene analyzed using cBioPortal with the Glioblastoma (TCGA, Pan Cancer Atlas) dataset. **(F)** Correlation between USP5 Expression and Immune Infiltration in GBM. Spearman correlation between the generalized expression of USP5 and the infiltration scores of various immune cell types in GBM. Purple shades represent a negative correlation. Red shades represent a positive correlation. (\*:  $p$  value  $< 0.05$ , #:  $FDR < 0.05$ ). **(G)** Immune Cell Abundance and USP5 Copy Number Variation in GBM. This figure, consisting of two volcano plots, illustrates the change in immune cell abundance in glioblastoma (GBM) tumors with a USP5 copy number variation (CNV) compared to those with a wild-type (WT) gene.

### Microarray based comparison of gene expression data from GEO expression omnibus dataset between USP5 and MGMT

Furthermore, to understand the correlation between the mRNA expression of USP5 and MGMT in glioblastoma, we analyzed publicly available microarray GEO datasets ( $N=145$ ; GSE43378, GSE4412, GSE279426, GSE13041). Heatmap analysis discovered the positive correlation expression patterns of USP5 and MGMT across multiple glioblastoma samples ( $n=145$ ), with visible clustering of cases showing high or low expression of the two genes. Furthermore, Correlation analysis was done using linear regression model, which showed a positive correlation between USP5 and MGMT expression. This trend indicates that increased USP5 expression is accompanied by higher MGMT at the transcript level. To further assess this, samples were distributed into high and low expression groups (HIGH =  $z$ -score  $> 0.2$  & LOW =  $z$ -score  $< 0.2$ ). The contingency table showed that 31 samples with high USP5 expression also exhibited high MGMT expression, 26 with low MGMT. Interestingly, among low USP5 cases, 32 showed high MGMT, while 56 had low MGMT. The Fisher's exact test indicated a statistically significant association between USP5 and MGMT expression ( $P=0.04$ ). This suggests a positive correlation between USP5 and MGMT expression with Pearson coefficient value  $r=0.2083$  ( $p$ -value: 0.012) in glioblastoma, supporting a potential regulatory or co-expression relationship between the two genes (Fig. 1c(i)).

Kaplan–Meier survival analysis revealed a distinct relationship between USP5 and MGMT co-expression and patient prognosis. In the positive correlation analysis, patients exhibiting concomitant low USP5–MGMT expression demonstrated better overall survival as compared to the high USP5–MGMT group. This pattern suggests that upregulation of USP5 alongside upregulation of MGMT may be associated with poorer clinical outcomes. Conversely, in the negative correlation analysis, the overall survival graph indicates that individuals with high USP5–low MGMT expression show comparatively better survival outcomes as compared to the group with low USP5–high MGMT. The survival curve for this group declines more gradually, maintaining a larger number of patients at risk during early and mid-time intervals. Together, these findings indicate that high MGMT expression in patients leads to poorer overall survival, indicating that elevated MGMT levels are associated with an adverse prognostic impact & concomitant USP5 and MGMT expression shows an effect on the overall survival where high expression of both USP5 & MGMT shows poor overall survival in patients than sample group with lower expression of both USP5 and MGMT, implicating USP5 and MGMT as potential modulators of glioma aggressiveness and prognosis (Fig. 1c(ii)).

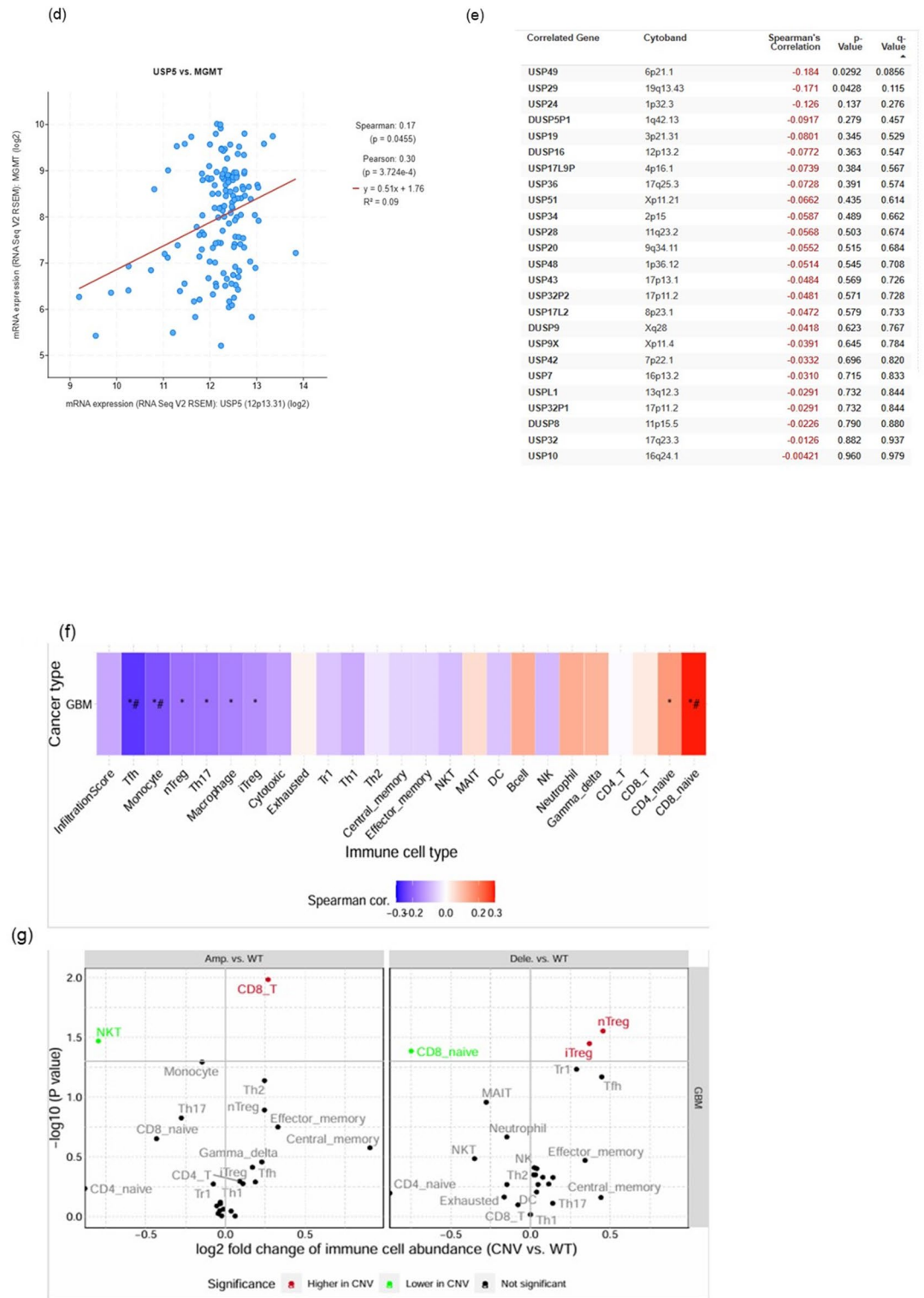


Fig. 1. (continued)

**The correlation between deubiquitinating enzymes USP5 and USP8 with MGMT across existing glioma tumor sample databases using cBioPortal**

The dataset of 592 glioma patients from the cBioPortal repository was analyzed to assess gene correlation between MGMT and Ubiquitin Specific Protease (USP). The mRNA correlation analysis using the TCGA dataset revealed a significant positive association between USP5 and MGMT expression, with a Pearson coefficient of 0.30, Spearman coefficient of 0.17, and p-value=0.04 (Fig. 1d), suggesting a cooperative relationship between USP5 and MGMT at the mRNA level in gliomas. In contrast, analysis of the broader USP family indicated

that most family members were negatively correlated with MGMT expression (Fig. 1e). Therefore, in continued studies, we selected USP5, a USP family protein, to demonstrate MGMT protein expression in temozolomide-resistant glioma cell lines.

### Correlation between USP5 expression and copy number variation and tumor immune microenvironment

An analysis of the USP5 gene's influence on the tumor immune microenvironment revealed several key findings. The GSVA heatmap indicated a positive correlation between USP5 expression and the infiltration of CD4 naïve cells, CD8 naïve cells, neutrophils, and Gamma\_delta cells. Conversely, a strong negative correlation was observed with Tfh (T follicular helper cells), Monocyte, nTreg (natural regulatory T cells), Th17 (T helper 17), and Macrophage cells, suggesting that higher USP5 expression is associated with a decrease in the abundance of these specific immune cell types (Fig. 1f).

Further investigation into the impact of USP5 copy number variation (CNV) on immune cell abundance showed distinct patterns. In tumors with USP5 amplification (Amp.), there was a significant increase in the abundance of CD8 T cell and NKT cells compared to the wild-type (WT) group. In contrast, tumors with USP5 deletion (Dele.) exhibit a significant increase in the abundance of nTreg, iTreg (induced regulatory T cells), and CD8 naïve cells compared to the WT group. These results indicate that USP5 CNV is associated with significant, and sometimes opposing, changes in the abundance of specific immune cell types (Fig. 1g).

### Expression analysis of deubiquitinating enzymes in Temozolomide acquired resistance in U87 TMZ and LN229 TMZ resistant cell line

Furthermore, the U87MG and LN229 cell lines were forced to grow from lower concentrations of 50  $\mu\text{M}$  to higher concentrations of 400  $\mu\text{M}$  temozolomide and demonstrated TMZ resistance. Temozolomide is the standard chemotherapy drug used to treat glioma that causes cell cycle arrest at the G2/M phase<sup>26</sup>. We have previously reported that our TMZ-resistant cell line models did not show G2/M cell cycle phase arrest upon temozolomide treatment, whereas naïve U87 and LN229 glioma cells showed G2/M phase arrest upon temozolomide treatment<sup>25</sup>. Furthermore, we analyzed DUB protein expression levels of USP7, USP8, USP10, USP1, USP14, and USP5, along with TNFAIP3 protein and MGMT protein, in U87 TMZ-resistant cells as well as in LN229 TMZ-resistant cell lines. Protein expression of USP1 was initially upregulated up to 200  $\mu\text{M}$  TMZ resistance in U87MG cells, which was further downregulated at the highest dose of TMZ-established resistant cells (400  $\mu\text{M}$ ), whereas in LN229 TMZ-resistant cells, USP1 was downregulated in a dose-dependent manner. USP7 was downregulated with increasing doses of TMZ resistance in U87 TMZ-resistant cells, whereas it was upregulated in LN229 TMZ-resistant cells. Deubiquitinating enzymes USP5, USP8, and USP10 were upregulated with increasing dosages of acquired TMZ resistance in both U87 TMZ-resistant and LN229 TMZ-resistant glioma cells, whereas USP14 showed no change in protein expression in either TMZ-resistant glioma cell line. TNFAIP3, a dual enzyme that functions as both a deubiquitinase and ubiquitinase, was upregulated with increasing doses of acquired TMZ resistance in both U87 TMZ-resistant and LN229 TMZ-resistant glioma cells (Fig. 2a & b). MGMT, a poor prognosis marker, was upregulated in U87 TMZ-resistant glioma cells with increasing doses of acquired temozolomide resistance. This dataset concludes that TMZ-resistant glioma cells show elevated protein expression of different DUBs: USP5, USP10, USP8, TNFAIP3, and MGMT. Additionally, we analyzed the expression of LC3B cleavage (an autophagy marker) and apoptotic mitochondrial protein SMAC. The expression of both LC3B cleavage and SMAC was inversely correlated (Fig. 2c), suggesting that temozolomide resistance leads cells to become more autophagic.

### USP5 and USP8 knockdown induces apoptosis and regulates MGMT expression through proteasomal degradation in temozolomide-resistant glioma cells

In one of our previously published studies, individual USP5 and USP8 knockdown in naïve U87 glioma cells demonstrated a lack of apoptosis inhibition, whereas apoptosis induction was revealed only upon co-knockdown of both USP5 and USP8<sup>24</sup>. In the present study, we knocked down USP5 and USP8 using two distinct specific siRNA sequences to optimize knockdown efficiency in U87 TMZ-resistant glioma cells. For USP5, both siRNA sequences demonstrated effective protein depletion; however, USP5 knockdown using both siRNAs resulted in compensatory USP8 upregulation, indicating functional crosstalk between these deubiquitinases. For USP8 targeting, the first siRNA sequence achieved approximately 20% knockdown efficiency, while the second siRNA sequence failed to produce measurable protein reduction (Fig. 3a). Consequently, all subsequent USP8 knockdown experiments utilized the first USP8 siRNA sequence that demonstrated functional efficacy.

Following successful siRNA-mediated knockdown, we analyzed protein expression of SMAC and autophagic marker LC3B in USP5 and USP8 knockdown U87 TMZ-resistant glioma cells. Knockdown of USP5 and USP8 resulted in upregulation of apoptotic inducer SMAC protein expression along with upregulated LC3B cleavage, leading to increased LC3II protein formation, which signifies autophagic cell death (Fig. 3a). These findings suggest that USP5 and USP8 function as survival factors in resistant cells by suppressing cell death mechanisms.

U87 TMZ-resistant glioma cells are known to re-express the MGMT protein<sup>25</sup>. The expression of MGMT protein provides a DNA repair mechanism by removing the O6-methylguanine adduct from guanine added by the alkylating agent temozolomide<sup>27</sup>. Based on these initial observations of cell death pathway activation, we investigated whether deubiquitinase knockdown affected the resistance factor MGMT using immunofluorescence analysis. In control U87 TMZ-resistant glioma cells, MGMT was localized in the cytoplasm with a fluorescence intensity of 2.50, which after Bortezomib treatment accumulated inside the nucleus with a fluorescence intensity of 2.85. Furthermore, MGMT protein expression was significantly downregulated following USP5 and USP8 knockdown and remained localized in the cytoplasm, with fluorescence intensities decreasing to 1.2 and 1.45, respectively (Fig. 3b).

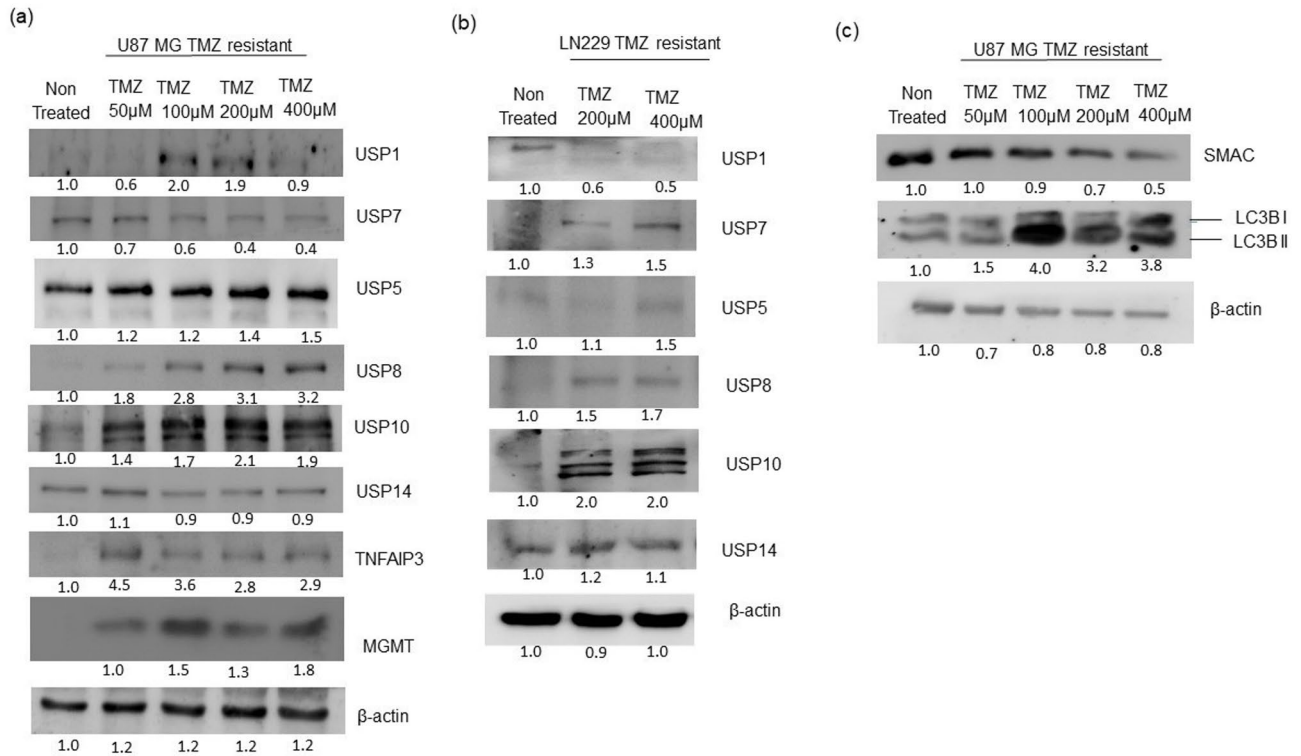


**Fig. 2.** Expression study of Deubiquitinating enzymes in Temozolomide resistant (U87 TMZ and LN229 TMZ resistant) glioma cells. **(A)** Immunoblot analysis showing deubiquitinating enzyme expression in U87 TMZ-resistant glioma cells.  $\beta$ -actin serves as loading control. Densitometry analysis was performed after normalization to  $\beta$ -actin. Blots were cut prior to hybridization with primary antibody. Representative blots are cropped images. Full-length original uncropped blots are provided in “Supplementary File Uncropped Images.” **(B)** Immunoblot analysis showing deubiquitinating enzyme expression in LN229 TMZ-resistant glioma cells.  $\beta$ -actin serves as loading control. Densitometry analysis was performed after normalization to  $\beta$ -actin. Blots were cut prior to hybridization with primary antibody. Representative blots are cropped images. Full-length original uncropped blots are provided in “Supplementary File Uncropped Images.” **(C)** Immunoblot analysis showing SMAC and LC3B protein expression in U87 TMZ-resistant glioma cells.  $\beta$ -actin serves as loading control. Densitometry analysis was performed after normalization to  $\beta$ -actin. Blots were cut prior to hybridization with primary antibody. Representative blots are cropped images. Full-length original uncropped blots are provided in “Supplementary File Uncropped Images.”

To determine the mechanism underlying this MGMT downregulation, we treated the knockdown cells with Bortezomib, a proteasome inhibitor. Following USP5 knockdown along with Bortezomib treatment, the MGMT protein accumulated in both cytoplasm and nucleus with fluorescence intensity increasing to 3.4, whereas no such accumulation of MGMT protein was observed in USP8 knockdown with Bortezomib treatment, demonstrating that USP5 prevents MGMT degradation through the proteasomal pathway (Fig. 3b). The relative fluorescence intensity data for MGMT across different treatment conditions are presented in the accompanying graph.

To confirm these immunofluorescence observations, we performed Western blot analysis of MGMT expression following USP5 and USP8 knockdown in U87 TMZ and LN229 TMZ glioma cells. In U87 TMZ-resistant cells, we observed significant downregulation of MGMT protein expression after USP5 and USP8 knockdown, validating our immunofluorescence findings. Additionally, USP10 protein levels consistently decreased upon either USP5 or USP8 depletion, suggesting USP10 functions as a downstream effector in this regulatory cascade (Fig. 3c). In contrast, LN229 TMZ-resistant glioma cells exhibited complete absence of MGMT protein expression under all conditions tested (Fig. 3d), as validated against T98G cells which served as a positive control for MGMT expression (Supplementary File- Uncropped Image Fig. 3d).

Having established the molecular mechanisms underlying deubiquitinase function, we confirmed the functional consequences through flow cytometric analysis of cell death. In U87 TMZ-resistant cells, USP5 siRNA treatment induced significant apoptosis with 9.66% early apoptosis, 85.44% late apoptosis, and 0.26% necrosis, while USP8 siRNA resulted in 7.98% early apoptosis, 90.03% late apoptosis, and 0.21% necrosis. Control scrambled siRNA demonstrated minimal cell death with 4.21% early apoptosis, 6.05% late apoptosis, and 1.88% necrosis, confirming the critical dependence of TMZ-resistant cells on elevated USP5 and USP8 levels for survival (Fig. 3e).

LN229 TMZ-resistant cells, despite lacking MGMT protein, showed equally significant responses to USP5 and USP8 knockdown. Control scrambled siRNA treatment resulted in minimal baseline cell death (0.3% early apoptosis, 0.2% late apoptosis), while USP5 knockdown induced 12.5% early apoptosis, 6.5% late apoptosis, and

13.9% necrosis. USP8 depletion led to 13.9% early apoptosis, 14.5% late apoptosis, and 16.9% necrosis (Fig. 3f). These results demonstrated that even in the absence of MGMT protein, LN229 TMZ-resistant cells remain critically dependent on USP5, USP8, and USP10 for survival, indicating that these deubiquitinases promote resistance through multiple mechanisms beyond MGMT stabilization. This discovery suggests that targeting deubiquitinases could provide broad therapeutic benefit across different resistance phenotypes.

### Immunofluorescence staining confirmed MGMT localization with USP5

Immunofluorescence staining was performed to determine the expression and spatial distribution of MGMT (red), USP5 (green), and nuclei (blue) in U87 TMZ-resistant glioma cells and Grade IV GBM tumor patient tissue. Initially, we examined formalin-fixed Grade IV glioblastoma tumor sections to validate the clinical relevance of USP5-MGMT interaction. In tumor tissues, MGMT expression was highly abundant and widespread, displaying a dense distribution pattern throughout the tissue section. USP5 also demonstrated strong expression; however, regions with high-density USP5 expression co-localized with areas of high MGMT intensity (Fig. 4a). This clinical observation established the foundation for our mechanistic studies in cell culture models.

Subsequently, we analysed U87 TMZ-resistant glioma cells to examine the subcellular localization patterns. MGMT exhibited strong cytoplasmic localization with very low nuclear distribution in the majority of U87 TMZ-resistant cells. Similarly, USP5 displayed cytoplasmic staining, with some cells presenting punctate or aggregated expression patterns in the nucleus. Notably, areas of yellow fluorescence in merged images demonstrated strong co-localization of MGMT and USP5, predominantly in the cytoplasm and partially in perinuclear regions. DAPI staining confirmed intact nuclei, facilitating accurate assessment of intracellular localization.

To investigate USP5's role in MGMT regulation, USP5 was knocked down in TMZ-resistant U87 cells, and identical immunofluorescence analysis was performed. A significant decrease in green fluorescence intensity confirmed effective USP5 knockdown. However, MGMT remained prominently inside the cytoplasm along with downregulation, though substantial loss of co-localization (yellow signal) was observed compared to controls (Fig. 4b). Collectively, these results from both *in vitro* studies and GBM patient samples provide consistent evidence of USP5 and MGMT co-expression and co-localization, suggesting a potential regulatory interaction.

Furthermore, the interaction between USP5 and MGMT was examined using co-immunoprecipitation (Co-IP) assays. Immunoprecipitation of MGMT was performed in U87 TMZ-resistant and T98G (MGMT-positive) glioma cell lines to demonstrate interaction with USP5. Interestingly, MGMT was predominantly observed in SUMOylated, higher molecular weight modified forms in the presence of temozolomide under resistant conditions, suggesting that USP5 may influence MGMT regulation through post-translational modifications (Supplementary Fig. 1). This interaction implies a potential mechanism whereby USP5 could stabilize or modulate MGMT activity, thereby contributing to temozolomide resistance in glioma.

### Knockdown of deubiquitinating enzyme USP8 downregulates MGMT protein expression independent of USP5 in TMZ resistant glioma cells

Furthermore, to determine whether MGMT upregulation in TMZ-resistant glioma cells is dependent on deubiquitinating enzymes USP5 or USP8, we performed USP8 knockdown in U87 TMZ-resistant glioma cells, followed by Bortezomib treatment (50  $\mu$ M) for 24 h, and conducted immunofluorescence staining for MGMT (red) and USP5 (green).

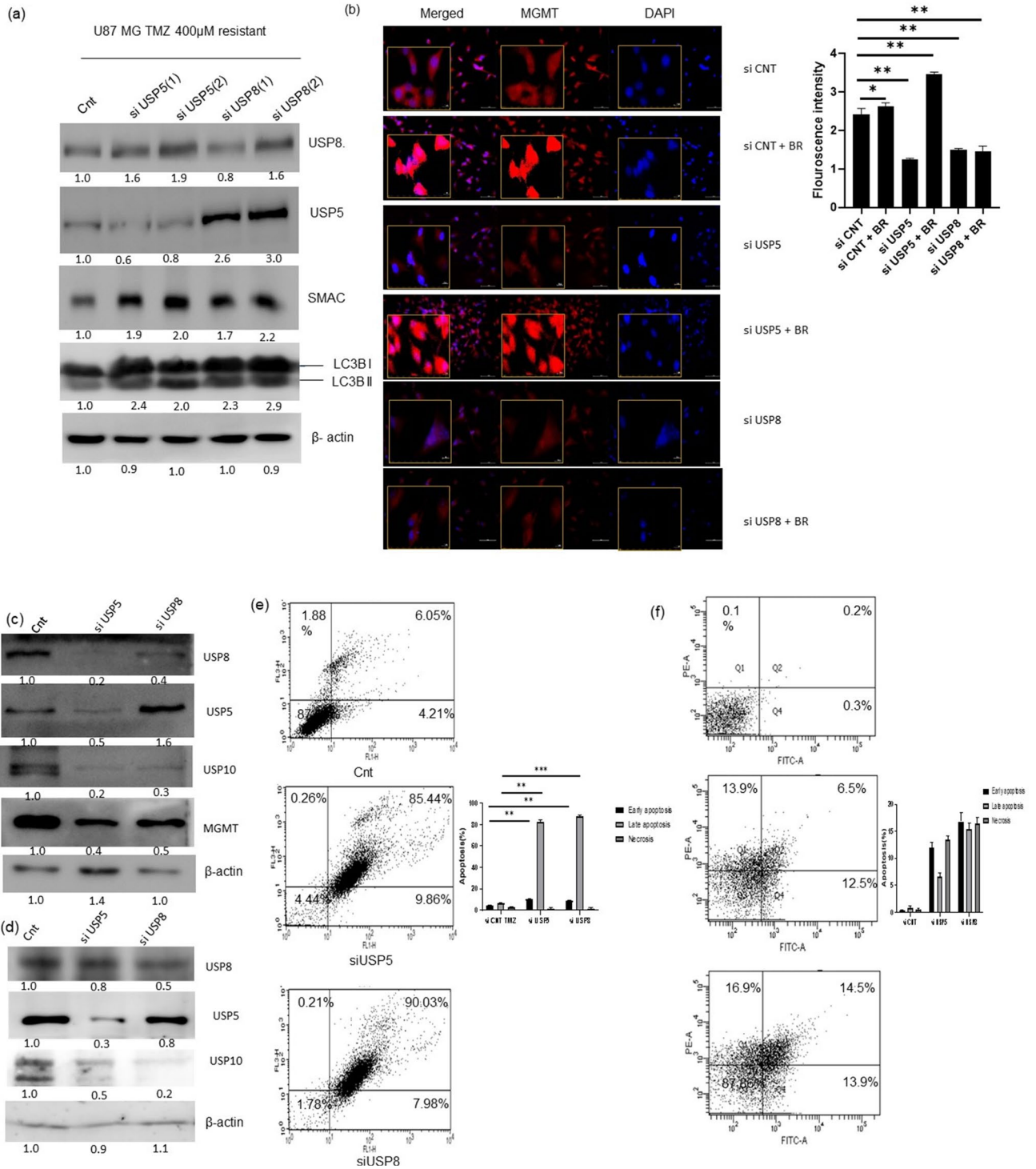
In U87 TMZ-resistant control cells, strong co-localization of MGMT (red) and USP5 (green) was observed, resulting in prominent yellow fluorescence, particularly in the cytoplasm. Following Bortezomib treatment, both MGMT and USP5 protein expression remained prominent in the cytoplasm without much accumulation, observed in confocal microscopy images.

In USP8 knockdown cells, MGMT expression was markedly reduced compared to control cells and present in the cytoplasm, whereas USP5 protein was prominently seen inside the nucleus only and due to this the co-localization between MGMT- USP5 lost in the cytoplasm. However, in, USP8 knockdown upon Bortezomib treatment showed the accumulation of MGMT in the cytoplasm, and with partial restoration of USP5 expression in cytoplasm, due to re-localisation of USP5 from nucleus to cytoplasm with accumulated MGMT in cytoplasm confirm their co-localisation in the presence of proteasomal inhibitor Bortezomib (Fig. 5a). These data indicate that USP8 plays a critical role in maintaining MGMT expression levels. USP8 silencing alone leads to visible MGMT reduction through proteasomal degradation pathway. A schematic representation of MGMT regulation by USP5 and USP8 in U87 TMZ-resistant glioma cells is depicted in Fig. 5b.

Collectively, these findings support the concept that targeting USP8 represents an effective strategy to downregulate MGMT, a key resistance factor in glioma.

### Overexpression of USP5 upregulates the MGMT expression in U87 MG glioma cells and HEK 293T cells

Furthermore, western blotting was performed after transient overexpression of USP5 plasmid at its two dosage 2  $\mu$ g and 4  $\mu$ g in HEK 293T cells. A marked increase in USP5 protein expression was seen in transiently overexpressed USP5 HEK 293T cells compared to pBABE control vector. Moreover, MGMT protein expression was upregulated in USP5 overexpressed protein HEK293T cells (Fig. 5c). Moreover, USP5 was also over expressed in U87 MG glioma cells. In untreated U87 MG cells, USP5 was present but MGMT expression was absent. Treating U87 MG cells with temozolomide alone, or with the control vector, did not lead to detectable MGMT expression, and USP5 levels remained largely unchanged. Interestingly, when USP5 was overexpressed in U87 MG cells followed by temozolomide treatment, both USP5 and MGMT levels were strongly induced,



with marginal upregulation of USP8. As a positive control, T98G cells showed the expected high basal MGMT expression (Fig. 5d). This concludes that overexpression of USP5 has relevant up-regulatory effect over MGMT not only in glioma cells but also in HEK 293T cells.

### Discussion

Temozolomide is the most preferred approved chemotherapy for glioma patients. In glioma patients resistance to alkylating drugs Temozolomide confer with enhancement in MGMT expression<sup>28</sup>. Epigenetic deregulation with subsequent MGMT expression and resistance occurrence adopted as predictor for Temozolomide treatment towards overall patient survival. Despite this, Temozolomide is the only current treatment option with dismal outcome, where patient median survival was only extended to two years<sup>1</sup>.

Additionally, keeping the MGMT degradation and stabilization would be another strategy to study its abundance as first line resistance marker to repair the Temozolomide mediated DNA break point consecutively.

◀ **Fig. 3.** Deubiquitinating enzyme USP5 and USP8 knockdown results into apoptotic stimuli in U87 TMZ and LN229 TMZ resistant glioma cells. (A) Immunoblot analysis showing USP5, USP8, SMAC, and LC3B expression following USP5 and USP8 knockdown using two different siRNAs. USP5 knockdown results in USP8 downregulation, while USP8 knockdown leads to USP5 upregulation, along with increased expression of pro-apoptotic protein SMAC.  $\beta$ -actin serves as loading control. Blots were cut prior to hybridization with primary antibody. Representative blots are cropped images. Full-length original uncropped blots are provided in “Supplementary File Uncropped Images.” (B) Immunofluorescence analysis showing MGMT expression in U87 TMZ-resistant glioma cells following USP5 and USP8 knockdown and Bortezomib treatment for 24 h. MGMT (red) and nuclei counterstained with DAPI (blue). Graph shows fluorescence intensity quantification for respective treatments. Scale bar: 50  $\mu$ m. Data are expressed as mean  $\pm$  SE. \* $p < 0.05$ , \*\* $p < 0.01$ , \*\*\* $p < 0.001$ . (C) Immunoblot analysis showing USP10, USP5, USP8, and MGMT expression in U87 TMZ-resistant glioma cells following USP5 and USP8 knockdown. USP10 and MGMT expression are downregulated in both USP5 and USP8 knockdown U87 cells.  $\beta$ -actin serves as loading control. Densitometry analysis was performed after normalization to  $\beta$ -actin. Blots were cut prior to hybridization with primary antibody. Representative blots are cropped images. Full-length original uncropped blots are provided in “Supplementary File Uncropped Images.” (D) Immunoblot analysis showing USP10, USP5, USP8, and MGMT expression in LN229 TMZ-resistant glioma cells following USP5 and USP8 knockdown. T98G cells serve as positive control for MGMT expression. USP10 expression is downregulated in both USP5 and USP8 knockdown LN229 cells, which lack endogenous MGMT protein.  $\beta$ -actin serves as loading control. Densitometry analysis was performed after normalization to  $\beta$ -actin. Blots were cut prior to hybridization with primary antibody. Representative blots are cropped images. Full-length original uncropped blots are provided in “Supplementary File Uncropped Images.” (E) Flow cytometric analysis of apoptosis in U87 TMZ-resistant glioma cells following USP5 and USP8 knockdown using specific siRNAs. Cells were analyzed 72 h post-transfection using Annexin V-APC/Propidium Iodide staining to determine early apoptosis, late apoptosis, and necrosis. Graph shows percentage of cell death (early apoptosis, late apoptosis, necrosis) for each treatment condition. Data are expressed as mean  $\pm$  SD from three independent experiments. \* $p < 0.05$ , \*\* $p < 0.01$ , \*\*\* $p < 0.001$ . (F) Flow cytometric analysis of apoptosis in LN229 TMZ-resistant glioma cells following USP5 and USP8 knockdown using specific siRNAs. Cells were analyzed 72 h post-transfection using Annexin V-APC/Propidium Iodide staining to determine early apoptosis, late apoptosis, and necrosis. Graph shows percentage of cell death (early apoptosis, late apoptosis, necrosis) for each treatment condition. Data are expressed as mean  $\pm$  SD from three independent experiments. \* $p < 0.05$ , \*\* $p < 0.01$ , \*\*\* $p < 0.001$ .

Moreover, the scenario after Temozolomide treatment not only enhances MGMT expression but also allows the upregulation of several key Deubiquitinating enzyme family proteins in acquired Temozolomide resistant U87 and LN229 cells. Notably, in vitro studies in U87 MG TMZ-resistant and LN229 TMZ-resistant cell lines revealed consistent upregulation of the USP5, USP8, USP10, and TNFAIP3 and MGMT proteins in TMZ-resistant cell lines, indicating their strong involvement along with MGMT in the TMZ-resistant phenotype. This upregulation of DUBs suggests an adaptive cellular response in which these DUBs may stabilize proteins for survival and resistance mechanisms. These unseen overexpressed DUB's family proteins in cancer distinctly affect the multiple pathways mediating chemo resistance by positively regulating the Epithelial to mesenchymal transition (EMT), reported till date in presence of USP10, USP22, USP37, USP29<sup>29,30</sup>. USP10 overexpression promotes mesenchymal state in glioma through stabilization of RUNX1 and SLUG1 protein<sup>29,31</sup>. The upregulation of USP10 increases the expression of mesenchymal markers such as YKL-40, MET, and COL5A1 in glioma to promote invasive mesenchymal state<sup>29</sup>. Interestingly, in our study knockdown of USP5 and USP8 downregulates the protein expression of UPS10 in U87 TMZ resistant glioma suggesting a more prominent approach to inhibit not only the EMT transition in glioma but also the MGMT resistance factor in MGMT positive glioma cells.

Recently, we published hnRNPA1 abundance in Temozolomide resistant glioma cells promotes resistance factor, observed not only due to MGMT but also because of gradual increase in SF2/ASF1 splice factor protein, which lead to hnRNPA1 overexpression with relative upregulation of hnRNPA1 higher isoform<sup>25</sup>. Therefore, knock down of SF2/ASF1 or hnRNPA1 higher isoform suppresses MGMT expression in Temozolomide resistant U87MG glioma cells. Since, MGMT expression in LN229 TMZ resistant cells is absent. Therefore, present study extended further to highlight few of deubiquitinating enzymes family protein per se, which were seen more common in between both U87 TMZ as well as in LN229 TMZ resistant cells. We have already published before, that knocking down of USP5 or USP8 didn't induce apoptosis, estimated with various apoptosis assays as well as flow cytometry Annexin V/PI staining, where we identified that the co-knockdown of USP5 and USP8 is important. But in present study Temozolomide resistant U87 and LN229 TMZ cell seemed to be addicted towards USP5 or USP8, come back to become sensitive towards absence of USP5 at least in presence of Temozolomide<sup>24</sup>. The knocking down of USP5 using its specific siRNA prominently induces apoptosis in both of the TMZ resistant cell lines along with down regulation of USP10 protein. However, since LN229 glioma cell non expressing the MGMT even after escalated high dosage of Temozolomide exposure didn't reveal any MGMT factor, but in U87MG upon Temozolomide exposure promotes MGMT were seen USP5 dependent in present study substantiated by USP5 knock down studies also indicates USP5 supports MGMT co-localization across the cell body from nucleus to cytosol distribution. Our study further has extended the USP5 and MGMT

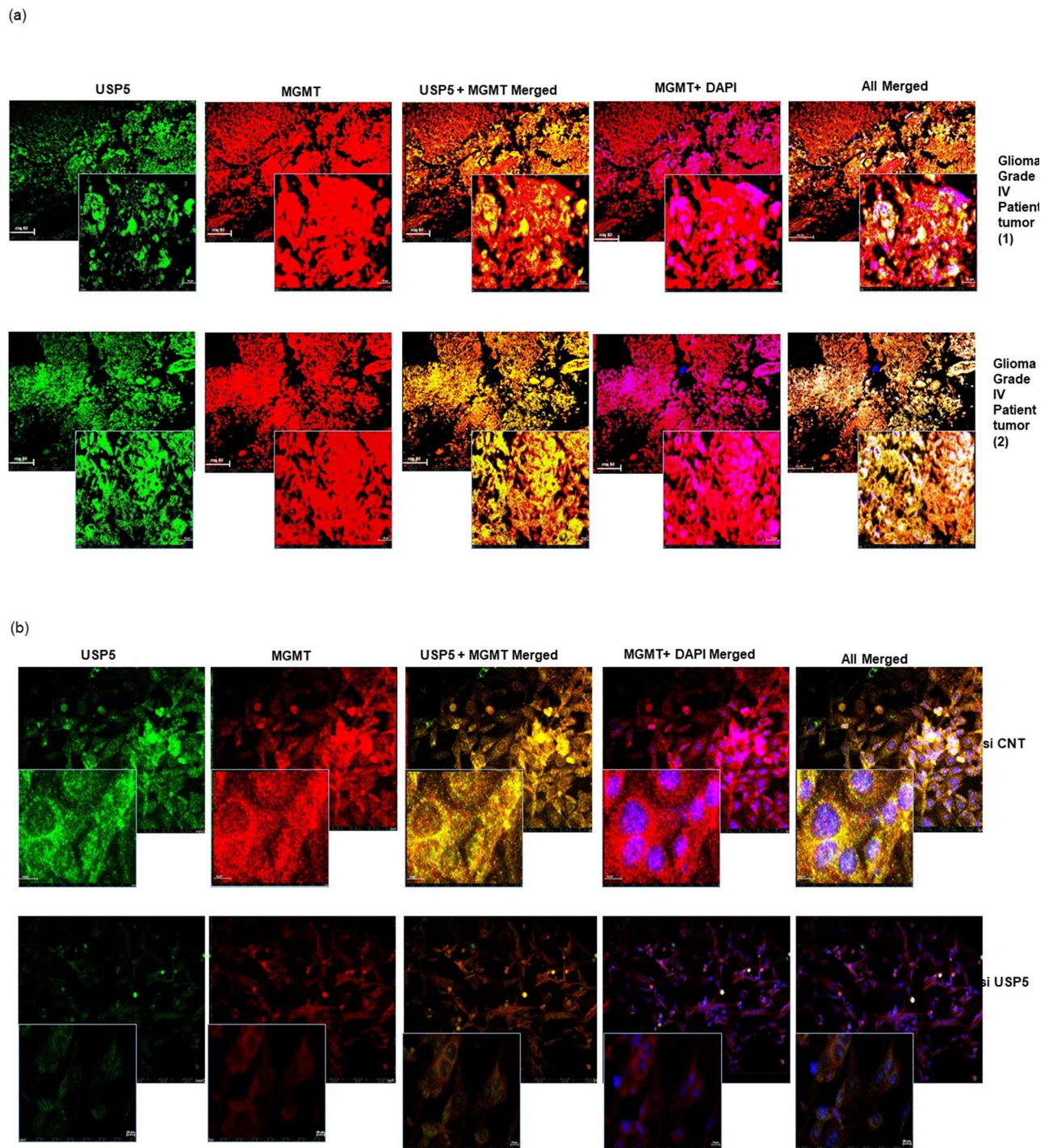
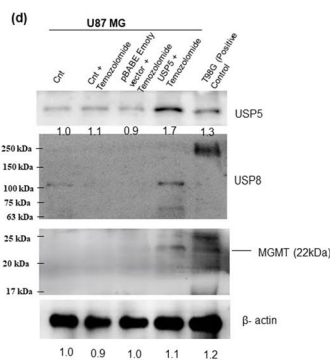
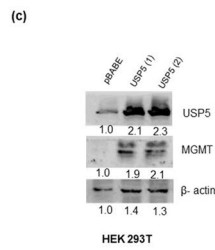
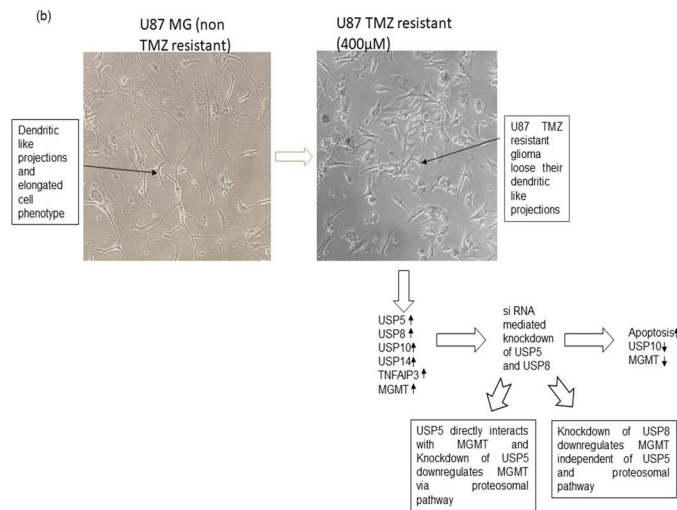
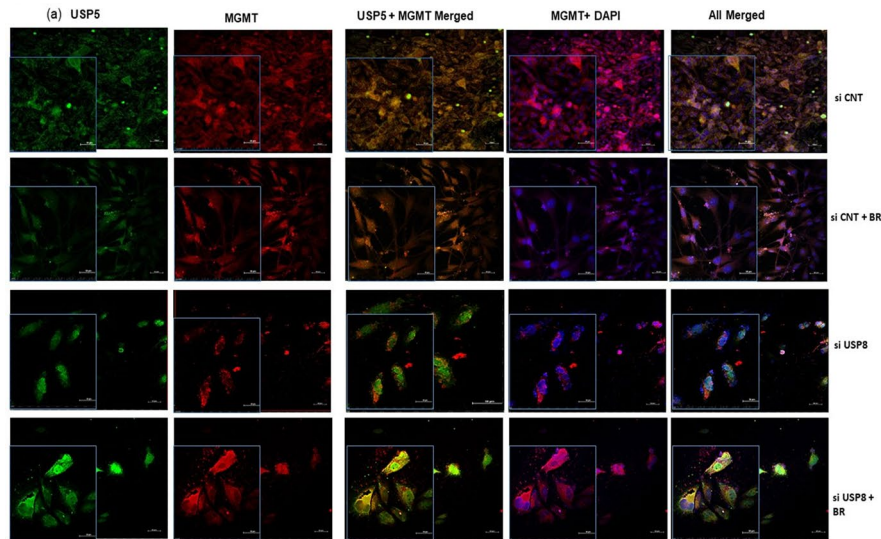


**Fig. 4.** Immunofluorescence staining based study of USP5 and MGMT localization in Glioma Grade IV patient tumor sample and U87 TMZ resistant glioma cells. **(A)** Immunofluorescence analysis of USP5 and MGMT expression in two Grade IV glioma tumor samples. MGMT (red), USP5 (green), and nuclei counterstained with DAPI (blue). Yellow indicates co-localization of MGMT and USP5. Scale bar: 50  $\mu$ m; Insets: 10  $\mu$ m. **(B)** Immunofluorescence analysis showing USP5 and MGMT expression in U87 TMZ-resistant glioma cells following USP5 knockdown using specific siRNA. USP5 (green), MGMT (red), and nuclei counterstained with DAPI (blue). Yellow indicates co-localization of USP5 and MGMT. Scale bar: 50  $\mu$ m; Insets: 10  $\mu$ m.

co-localization and eventually the abundance of MGMT got affected by expression of USP5 low vs. high, has also affected the MGMT expression and its localization in GBM grade IV tumor slide. Where, two population of cells were clearly seen in GBM tumor slide describes the USP5 and MGMT are positively correlated but in low expressing USP5 appears along with less MGMT. The positive correlation study was also extended in



between USP5 and MGMT across TCGA acquired glioblastoma tissue samples. This study further emphasizes the glioblastoma with high MGMT expression is dependent upon USP5 expression.

Most importantly our study identifies deubiquitinating enzyme USP8 as a new and independent regulator of MGMT in TMZ-resistant glioma. While cBioportal analyses did not find a correlation between USP8 mRNA and MGMT, whereas our experiments showed that knocking down USP8 significantly lowered MGMT protein levels without affecting USP5 expression. Immunofluorescence analysis indicated that the loss of USP8 reduced MGMT-USP5 co-localization. This finding highlights USP8's crucial role in maintaining MGMT levels, independent of USP5 activity. Moreover, USP8 knockdown co-treating with Bortezomib, a proteasome inhibitor, led to a more significant decrease in MGMT levels. This suggests that USP8 regulates MGMT expression apart from proteosomal pathway. Unlike USP5, which seems to directly interact with MGMT and regulates its degradation via proteosomal pathway, USP8 appears to influence MGMT through a different mechanism

◀ **Fig. 5.** Immunofluorescence staining using confocal microscope based study of USP5 and MGMT localization after deubiquitinating enzyme USP8 knockdown and Bortezomib treatment in U87 TMZ resistant glioma cells. (A) Confocal images showing MGMT and USP5 expression in U87 TMZ-resistant glioma cells following USP8 knockdown and Bortezomib treatment for 24 h. MGMT (red), USP5 (green), and nuclei counterstained with DAPI (blue). Yellow indicates co-localization of MGMT and USP5. Scale bar: 50  $\mu\text{m}$ ; Insets: 10  $\mu\text{m}$ . (B) Schematic representation of MGMT regulation by USP8 and USP5 in TMZ-resistant glioma. (C) Immunoblot analysis showing USP5 and MGMT expression in HEK293T cells following transient USP5 overexpression. Densitometric analysis was performed after normalization to  $\beta$ -actin. Blots were cut prior to hybridization with primary antibody. Representative blots are cropped images. Full-length original uncropped blots are provided in “Supplementary File Uncropped Images.” (D) Immunoblot analysis showing USP5, USP8 and MGMT expression in U87 MG glioma cells following transient USP5 overexpression. Untreated U87 MG cells express USP5 but lack detectable MGMT. Temozolomide treatment alone or with control vector does not induce MGMT expression. USP5 overexpression combined with temozolomide treatment markedly increases both USP5 and MGMT levels. T98G glioma cells serve as positive control for MGMT expression.  $\beta$ -actin serves as loading control. Blots were cut prior to hybridization with primary antibody. Representative blots are cropped images. Full-length original uncropped blots are provided in “Supplementary File Uncropped Images.”

that stabilizes the protein. In the tumor microenvironment (TME), the interaction between CD8 + T cells and tumor cells is a critical determinant of immune surveillance and cancer progression. CD8 + T cells express the inhibitory checkpoint receptor Programmed Cell Death Protein 1 (PD-1), which serves to regulate immune responses and prevent autoimmunity. Conversely, tumor cells can upregulate the expression of the ligand Programmed Death-Ligand 1 (PD-L1) as a primary mechanism of immune evasion. Research indicates that high MGMT expression in some cancers can also be linked to reduced immune cell infiltration and properties of immune evasion, suggesting a mechanism by which the tumor avoids detection and destruction by the immune system<sup>32</sup>. The binding of PD-1 on CD8 + T cells to PD-L1 on tumor cells delivers a powerful inhibitory signal, effectively “turning off” the T cell and preventing it from killing the cancer cell. This immune evasion mechanism contributes to tumor growth and poor patient outcomes.

Our findings demonstrate a direct link between USP5 expression and the immune microenvironment in glioblastoma (GBM), suggesting that both its expression gain or loss significantly shapes the tumor’s immune landscape. A negative correlation between general USP5 expression and the infiltration of cells like Tfh, monocytes, nTregs, Th17, and macrophages suggests that higher USP5 levels may be associated with a less favourable or immunosuppressive tumor microenvironment. This is particularly due to the lack of Tfh and nTregs, which are critical for regulating T-cell responses. The analysis of copy number variations (CNVs) further illuminates this complex relationship, showing distinct effects based on the type of genetic alteration. The increased abundance of CD8 + T and NKT cells in USP5 amplified tumors is particularly noteworthy. Both cell types are crucial for a robust anti-tumor immune response, with CD8 + T cells being the primary cytotoxic killers and NKT cells acting as an early line of defence. This observation is relevant in light of research demonstrating that USP5 can act as a deubiquitinase to stabilize the PD-L1 protein by removing ubiquitin chains that would otherwise mark it for degradation<sup>33</sup>. The PD-L1 protein, when expressed on the surface of tumor cells, binds to the PD-1 receptor on CD8 + T cells, leading to T-cell exhaustion and a suppressed anti-tumor immune response<sup>34</sup>. This mechanism suggests that the overall role of upregulated USP5 may be to foster an immunosuppressive environment where CD8 + T cells are present but rendered non-functional. The increased abundance of CD8 + T cells in our USP5-amplified GBM samples may thus reflect a compensatory mechanism where the tumor recruits these cells, but the elevated USP5 protein levels subsequently prevent them from effectively killing the tumor cells by stabilizing PD-L1. Conversely, the increased abundance of nTreg and iTreg cells in tumors with USP5 deletion points to a different outcome. These regulatory T cells are known for their immunosuppressive functions, actively dampening the anti-tumor immune response and promoting tumor growth. The concurrent increase in CD8<sub>naive</sub> cells suggests that while CD8 cells might be present, they are in a less activated or differentiated state and are unable to effectively combat the tumor. Given this complex interplay, immune checkpoint inhibitors (ICIs) targeting the PD-1/PD-L1 axis may be a promising therapeutic strategy to overcome this resistance. By blocking the PD-1/PD-L1 interaction, ICIs can activate CD8 + T cells, restoring their cytotoxic function and allowing them to kill cancer cells, thereby activating a more robust immune response. This approach could be particularly beneficial for tumors that rely on USP5-mediated stabilization of PD-L1 for immune evasion. Furthermore, targeting USP5 could serve as a novel therapeutic strategy to both modulate the tumor microenvironment and sensitize tumors to Temozolomide by downregulating the MGMT-mediated resistance effect.

Together, these results suggest that USP5 plays a multifaceted, context-dependent role in tumor immunity, where its amplification appears to be associated with a strategically favorable outcome for the tumor, while its deletion is linked to an immunosuppressive environment. This dual function indicates that USP5 may act as a critical regulator of immune cell recruitment and function in Glioblastomas.

## Data availability

The datasets used and/or analyzed during the current study are available from the corresponding author on reasonable request.

Received: 16 September 2025; Accepted: 12 January 2026

Published online: 24 January 2026

## References

- Wu, S. et al. PARP-mediated parylation of MGMT is critical to promote repair of temozolomide-induced O<sup>6</sup>-methylguanine DNA damage in glioblastoma. *Neuro-Oncology* **23**, 920–931. <https://doi.org/10.1093/neuonc/noab003> (2021).
- Everhard, S. et al. Identification of regions correlating MGMT promoter methylation and gene expression in glioblastomas. *Neuro-Oncology* **11**, 348–356. <https://doi.org/10.1215/15228517-2009-001> (2009).
- Malley, D. S. et al. A distinct region of the MGMT CpG Island critical for transcriptional regulation is preferentially methylated in glioblastoma cells and xenografts. *Acta Neuropathol.* **121**, 651–661. <https://doi.org/10.1007/s00401-011-0803-5> (2011).
- Brandes, A. A. et al. O<sup>6</sup>-methylguanine DNA-methyltransferase methylation status can change between first surgery for newly diagnosed glioblastoma and second surgery for recurrence: clinical implications. *Neuro-Oncology* **12**, 283–288. <https://doi.org/10.1093/neuonc/nop050> (2010).
- Felsberg, J. et al. Promoter methylation and expression of MGMT and the DNA mismatch repair genes MLH1, MSH2, MSH6 and PMS2 in paired primary and recurrent glioblastomas. *Int J. Cancer.* **129**, 659–670. <https://doi.org/10.1002/ijc.26083> (2011).
- Aasland, D. et al. Repair gene O<sup>6</sup>-methylguanine-DNA methyltransferase is controlled by SP1 and up-regulated by glucocorticoids, but not by Temozolomide and radiation. *J. Neurochem.* **144**, 139–151. <https://doi.org/10.1111/jnc.14262> (2018).
- Pitter, K. L. et al. Corticosteroids compromise survival in glioblastoma. *Brain* **139**, 1458–1471. <https://doi.org/10.1093/brain/aww046> (2016).
- Chumakova, A. & Lathia, J. D. Outlining involvement of stem cell program in regulation of O<sup>6</sup>-methylguanine DNA methyltransferase and development of Temozolomide resistance in glioblastoma: an editorial highlight for 'Transcriptional control of O<sup>6</sup>-methylguanine DNA methyltransferase expression and Temozolomide resistance in glioblastoma' on page 780. *J. Neurochem.* **144**, 688–690. <https://doi.org/10.1111/jnc.14280> (2018).
- Happold, C. et al. Transcriptional control of O<sup>6</sup>-methylguanine DNA methyltransferase expression and Temozolomide resistance in glioblastoma. *J. Neurochem.* **144**, 780–790. <https://doi.org/10.1111/jnc.14326> (2018).
- Hsu, S-H., Chen, S-H., Kuo, C-C. & Chang, J-Y. Ubiquitin-conjugating enzyme E2 B regulates the ubiquitination of O-methylguanine-DNA methyltransferase and BCNU sensitivity in human nasopharyngeal carcinoma cells. *Biochem. Pharmacol.* **158**, 327–338. <https://doi.org/10.1016/j.bcp.2018.10.029> (2018).
- Li, X. et al. Ubiquitination and degradation of MGMT by TRIM72 increases the sensitivity of uveal melanoma cells to Dacarbazine treatment. *CBM* **34**, 275–284. <https://doi.org/10.3233/CBM-210345> (2022).
- Panner, A. et al. Ubiquitin-Specific protease 8 links the PTEN-Akt-AIP4 pathway to the control of FLIPS stability and TRAIL sensitivity in glioblastoma multiforme. *Cancer Res.* **70**, 5046–5053. <https://doi.org/10.1158/0008-5472.CAN-09-3979> (2010).
- Wu, H-C. et al. USP11 regulates PML stability to control Notch-induced malignancy in brain tumours. *Nat. Commun.* **5**, 3214. <https://doi.org/10.1038/ncomms4214> (2014).
- Annibaldi, D. et al. Myc inhibition is effective against glioma and reveals a role for Myc in proficient mitosis. *Nat. Commun.* **5**, 4632. <https://doi.org/10.1038/ncomms5632> (2014).
- Zheng, H. et al. Pten and p53 converge on c-Myc to control Differentiation, Self-renewal, and transformation of normal and neoplastic stem cells in glioblastoma. *Cold Spring Harb. Symp. Quant. Biol.* **73**, 427–437. <https://doi.org/10.1101/sqb.2008.73.047> (2008).
- Sun, X-X. et al. SUMO protease SENP1 desumoylates and stabilizes c-Myc. *Proc. Natl. Acad. Sci. USA.* **115**, 10983–10988. <https://doi.org/10.1073/pnas.1802932115> (2018).
- Nagasaka, M. et al. The deubiquitinating enzyme USP17 regulates c-Myc levels and controls cell proliferation and Glycolysis. *FEBS Lett.* **596**, 465–478. <https://doi.org/10.1002/1873-3468.14296> (2022).
- Popov, N. et al. The ubiquitin-specific protease USP28 is required for MYC stability. *Nat. Cell. Biol.* **9**, 765–774. <https://doi.org/10.1038/ncb1601> (2007).
- Sun, X-X. et al. The nucleolar ubiquitin-specific protease USP36 deubiquitinates and stabilizes c-Myc. *Proc. Natl. Acad. Sci. USA.* **112**, 3734–3739. <https://doi.org/10.1073/pnas.1411713112> (2015).
- Pan, J. et al. USP37 directly deubiquitinates and stabilizes c-Myc in lung cancer. *Oncogene* **34**, 3957–3967. <https://doi.org/10.1038/onc.2014.327> (2015).
- Li, G. et al. USP5 sustains the proliferation of glioblastoma through stabilization of CyclinD1. *Front. Pharmacol.* **12**, 720307. <https://doi.org/10.3389/fphar.2021.720307> (2021).
- Yan, B. et al. A pan-cancer analysis of the role of USP5 in human cancers. *Sci. Rep.* **13**, 8972. <https://doi.org/10.1038/s41598-023-35793-2> (2023).
- Jiang, X. et al. E2F1-regulated USP5 contributes to the tumorigenic capacity of glioma stem cells through the maintenance of OCT4 stability. *Cancer Lett.* **593**, 216875. <https://doi.org/10.1016/j.canlet.2024.216875> (2024).
- Vashistha, V., Bhardwaj, S., Yadav, B. K. & Yadav, A. K. Depleting deubiquitinating enzymes promotes apoptosis in glioma cell line via RNA binding proteins SF2/ASF1. *Biochem. Biophys. Res. Rep.* **24**, 100846. <https://doi.org/10.1016/j.bbrep.2020.100846> (2020).
- Bhardwaj, S. & Sanjay, Yadav, A. K. Higher isoform of hnRNP1 confer Temozolomide resistance in U87MG & LN229 glioma cells. *J. Neurooncol.* **171**, 47–63. <https://doi.org/10.1007/s11060-024-04831-y> (2025).
- Filippi-Chiela, E. C. et al. Resveratrol abrogates the Temozolomide-induced G2 arrest leading to mitotic catastrophe and reinforces the Temozolomide-induced senescence in glioma cells. *BMC Cancer.* **13**, 147. <https://doi.org/10.1186/1471-2407-13-147> (2013).
- Pandith, A. A. et al. Concordant association validates MGMT methylation and protein expression as favorable prognostic factors in glioma patients on alkylating chemotherapy (Temozolomide). *Sci. Rep.* **8**, 6704. <https://doi.org/10.1038/s41598-018-25169-2> (2018).
- Qiu, Z-K. et al. Enhanced MGMT expression contributes to Temozolomide resistance in glioma stem-like cells. *Chin. J. Cancer.* **33**, 115–122. <https://doi.org/10.5732/cjc.012.10236> (2014).
- Qiu, W. et al. USP10 deubiquitinates RUNX1 and promotes proneural-to-mesenchymal transition in glioblastoma. *Cell. Death Dis.* **14**, 207. <https://doi.org/10.1038/s41419-023-05734-y> (2023).
- Chauhan, R. et al. Ubiquitin-specific peptidase 37: an important cog in the oncogenic machinery of cancerous cells. *J. Exp. Clin. Cancer Res.* **40**, 356. <https://doi.org/10.1186/s13046-021-02163-7> (2021).
- Ouchida, A. T. et al. USP10 regulates the stability of the EMT-transcription factor Slug/SNAI2. *Biochem. Biophys. Res. Commun.* **502**, 429–434. <https://doi.org/10.1016/j.bbrc.2018.05.156> (2018).
- Zhang, J. Y. et al. High MGMT expression identifies aggressive colorectal cancer with distinct genomic features and immune evasion properties. *J. Immunother. Cancer.* **13**, e011653. <https://doi.org/10.1136/jitc-2025-011653> (2025).
- Pan, J. et al. USP5 facilitates non-small cell lung cancer progression through stabilization of PD-L1. *Cell. Death Dis.* **12**, 1051. <https://doi.org/10.1038/s41419-021-04356-6> (2021).

34. Raskov, H., Orhan, A., Christensen, J. P. & Gögenur, I. Cytotoxic CD8 + T cells in cancer and cancer immunotherapy. *Br. J. Cancer.* **124**, 359–367. <https://doi.org/10.1038/s41416-020-01048-4> (2021).

### Acknowledgements

We would like to acknowledge Director, Dr. B.R. Ambedkar Center for Biomedical Research, University of Delhi for infrastructure facility and support of annual maintenance grant, Science Eng. Research Board (EMR/2015/009127) supported funds, New Delhi.

### Author contributions

SB, Sanjay, DS and LT did the experiments and drafted the manuscript; S.B, DS, BKY, AKY clinical samples correlation analysis, AKY conceived and generated the funds, interpreted the data, finalized the manuscript.

### Funding

Supported from Science Eng. Research Board, New Delhi (EMR/2015/009127).

### Declarations

### Competing interests

The authors declare no competing interests.

### Ethical approval and consent to participation

Protocols for the handling of human tissues and cells were approved by the Ethics committee of Dr. B.R Ambedkar Center for Biomedical Research (No.F.50 – 2/Eth.Com/ACBR/16/2379) and Rajiv Gandhi Cancer Institute and Research Centre (Res/SCM/17/2016/59).

### Additional information

**Supplementary Information** The online version contains supplementary material available at <https://doi.org/10.1038/s41598-026-36379-4>.

**Correspondence** and requests for materials should be addressed to A.K.Y.

**Reprints and permissions information** is available at [www.nature.com/reprints](http://www.nature.com/reprints).

**Publisher's note** Springer Nature remains neutral with regard to jurisdictional claims in published maps and institutional affiliations.

**Open Access** This article is licensed under a Creative Commons Attribution-NonCommercial-NoDerivatives 4.0 International License, which permits any non-commercial use, sharing, distribution and reproduction in any medium or format, as long as you give appropriate credit to the original author(s) and the source, provide a link to the Creative Commons licence, and indicate if you modified the licensed material. You do not have permission under this licence to share adapted material derived from this article or parts of it. The images or other third party material in this article are included in the article's Creative Commons licence, unless indicated otherwise in a credit line to the material. If material is not included in the article's Creative Commons licence and your intended use is not permitted by statutory regulation or exceeds the permitted use, you will need to obtain permission directly from the copyright holder. To view a copy of this licence, visit <http://creativecommons.org/licenses/by-nc-nd/4.0/>.

© The Author(s) 2026